Arabian Journal of Geosciences (2021) 14: 496
https://doi.org/10.1007/s12517-021-06862-5

ORIGINAL PAPER

Seasonal variability of mixed layer depth from Argo floats in the central Red Sea

Turki Metabe Alraddadi [1] · Mohammed Ali Alsaafani [1,2] · Alaa Mohammed Albarakati [1] · Cheriyeri Poyil Abdulla [1]

Received: 29 May 2020 / Accepted: 1 March 2021 / Published online: 12 March 2021
© Saudi Society for Geosciences 2021

Abstract

Argo floats are one of the eminent ocean observation systems which retrieve frequent measurements of temperature and salinity profiles in the remote marine environment and provide vital information about the world ocean with or without direct access to the human. The Argo floats available in the Red Sea are not well explored by the research community so far. In the present study, the temperature and salinity data from two Argo floats available in the central Red Sea for a period of 2 years are used to examine the mixed layer depth variability in the region. The mixed layer in the region is maximum during February associated with a decrease in static stability and shallowest during August due to an increase in static stability. A noticeable difference is observed in the existing mixed layer structure by the presence of eddies. The analysis of monthly mean thermal and haline structure showed that the warming of the surface layer is intense from March to August followed by cooling from September to February. The surface layer salinity increased from May to October and decreased in the following months. A noticeable east-west difference is observed in the thermal and haline structure, where the eastern side of the region is warmer by ~0.3 °C and less saline by ~0.1 PSU.

Keywords Mixed layer depth · Argo floats · Central Red Sea · Eddies · Temperature · Salinity

Introduction

The near surface quasi-homogenous layer is an imperative oceanographic variable in understanding the dynamics of the oceanic upper layer. The depth of this layer, often defined as mixed layer depth or ML, is vital in influencing the interaction between the atmosphere and ocean and associated physical and biological processes (Chen et al. 1994; Polovina et al. 1995). The availability of temperature and salinity profiles from Argo floats along with direct measurements improved our understanding on mixed layer regionally (D'Ortenzio et al. 2005; Zeng and Wang 2017; Abdulla et al. 2019) and globally (Gaube et al. 2019; Bessa et al. 2020; Sohail et al. 2020).

Red Sea is an important marginal sea, known for hot and saline characteristics, oriented north and northwest between 12°N to 30°N with about 2300 km long and 280 km wide on average, separated by the African and Asian continents, and plays an important role in the world's navigation routes, maritime transport, and connecting countries (Morcos 1970; Shanas et al. 2017; Abdulla et al. 2018). The Red Sea is connected to Indian Ocean through the strait of Bab-el-Mandab and the Gulf of Aden with surface and surface water exchange throughout the year. The influence of hot-arid climate surrounding the Red Sea, along with the lack of freshwater input, relatively strong evaporation, and presence of multiple number of eddies, results in complex dynamical processes in the region (Albarakati and Ahmad 2013; Zhai and Bower 2013; Zhan et al. 2014; Aboobacker et al. 2017; Abdulla et al. 2018).

The battery-powered Argo floats are capable to automatically profile remote ocean regions, where manual profiling is difficult for various reasons, up to a depth of 2000 m and for a period of 4 to 5 years. This advantage of Argo profiles in oceanographic research is not yet well explored in the Red Sea. The availability of in situ observation from platforms like

Responsible Editor: Zhihua Zhang

✉ Turki Metabe Alraddadi
talraddadi@kau.edu.sa

[1] Department of Marine Physics, Faculty of Marine Sciences, King Abdulaziz University, Jeddah, Saudi Arabia

[2] Department of Earth & Environmental Sciences, Faculty of Science, Sana'a University, Sana'a, Yemen

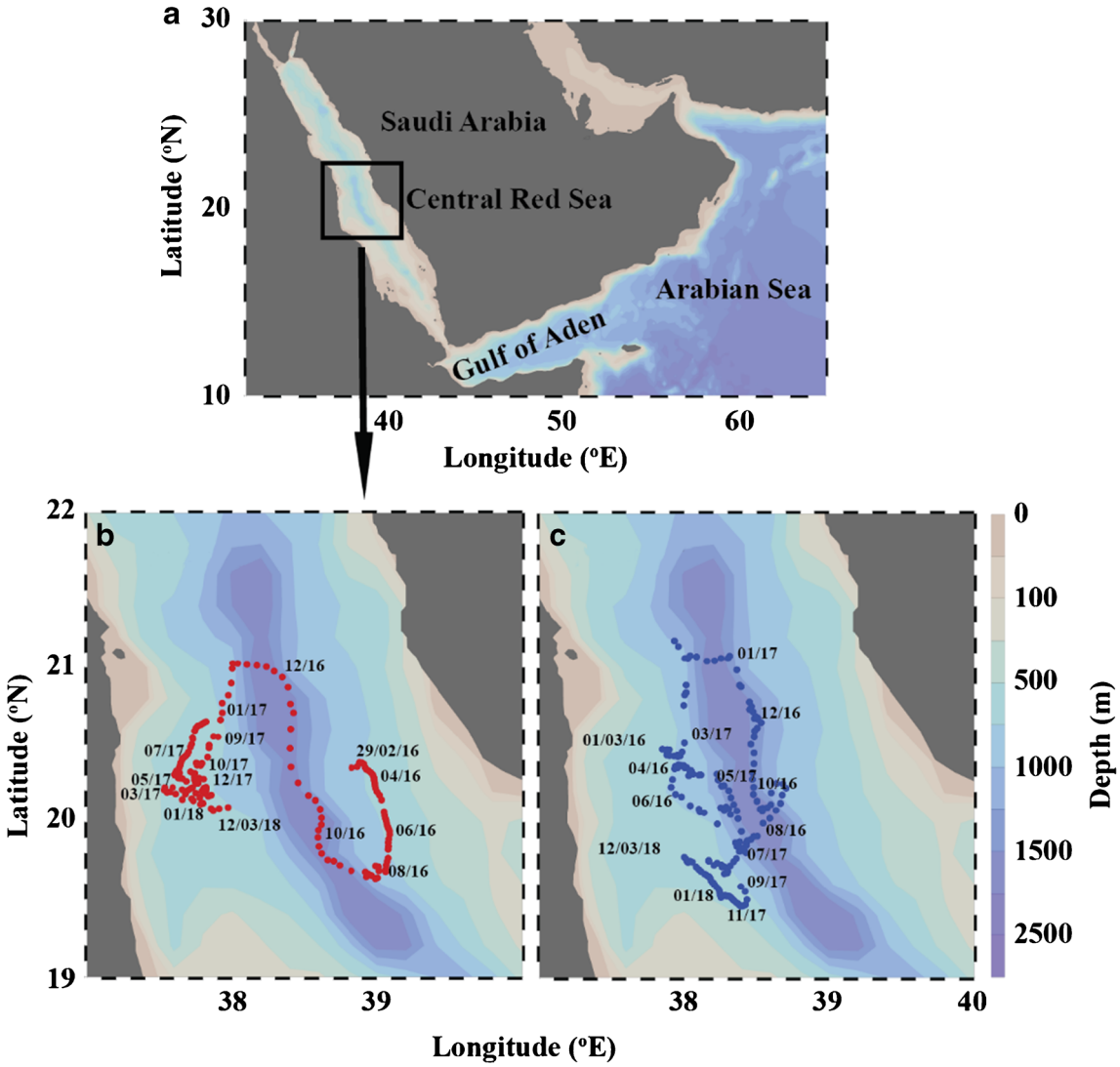

Fig. 1 **a** The geographical location of the central Red Sea, and the trajectory of the Argo floats **b** Argo-1 and **c** Argo-2

Argo floats will help in understanding ongoing physical mechanisms and be beneficial to validate ocean models in remote regions.

The information on the variability of MLD in the central Red Sea is restricted to very few studies mainly due to data scarcity. The availability of the Argo profiles is helpful in solving this issue to a large extent. The available study (Abdulla et al. 2018) has used temperature profiles only to describe MLD along the axial line of the Red Sea based on data from different sources which are scattered in both space and time. The present study is based on continuous profiles for a period of 2 years from simultaneously existed two Argo floats in the same region, with better temporal resolution of approximately 4 days or less. The data also covers both eastern and western coastal regions, which helped understand the east-west difference in hydrographic conditions and mixed layer structure. Comparing to the previous study, the present study has the advantage of better temporal resolution and coverage toward both eastern and western coastal regions. Further, the present study is based on both temperature and salinity profiles, while the previous was only based on temperature profiles. The sections in this paper are arranged as follows. "Data and methods" describes the datasets and methodology. "Results and discussion" discusses the temporal evolution of MLD variability in the central Red Sea and the role of local physical process on MLD variability. The summary of the results and conclusions are given in "Summary and conclusions."

Data and methods

Datasets

The Argo profiles used in the present study are received from Coriolis data center, which involves 7 institutes in operational oceanography in France that jointly do efforts to organize and maintain data acquisition in real time as well as delayed mode.

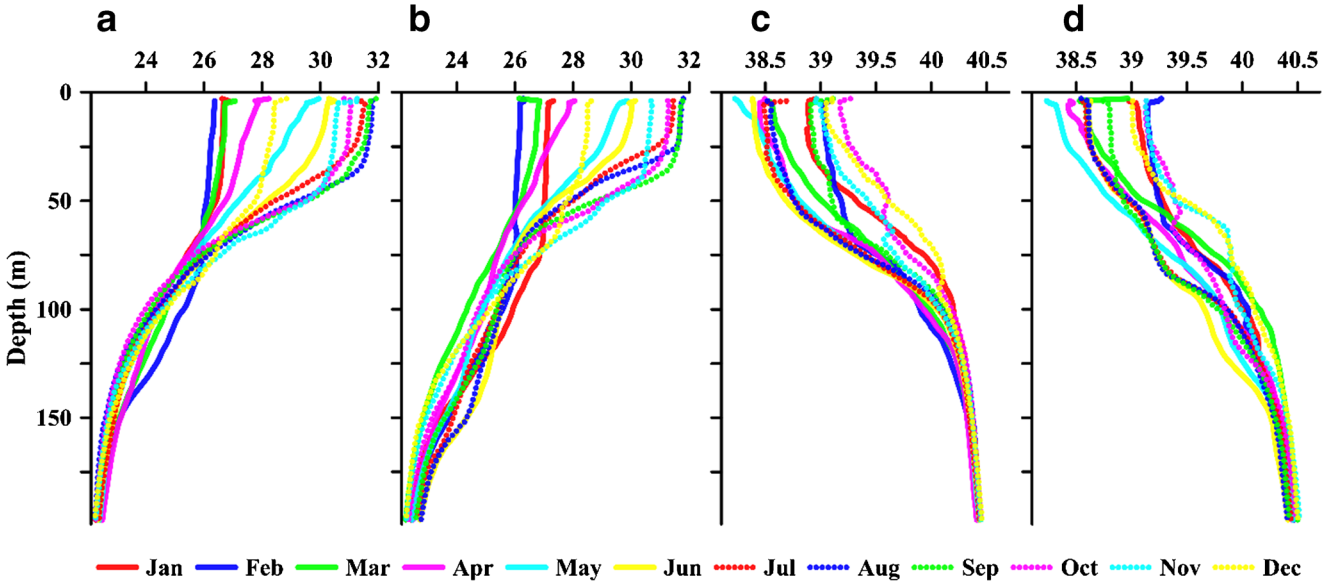

Fig. 2 The average monthly profiles of temperature and salinity for the 2-year period

The Argo profiles available in the Red Sea with an approximate interval of 4 days for a period of 2 years from 1 March 2016 to 15 March 2018 are used in the present study (http://www.coriolis.eu.org/Observing-the-Ocean/ARGO).

The sea level anomaly (SLA) data is available on daily time scale with spatial resolution of 0.25° × 0.25° from AVISO data center. The data is available from 1992 to present. For more information on AVISO sea level anomaly merged product, please refer to LaTraon and Dibarboure (1999) and Ducet et al. (2000). The SLA data is downloaded from ftp://ftp.aviso.altimetry.fr/global/delayed-time/grids/msla/all-satmerged/h/.

Methods

The Argo data is quality checked following Gould (2005). Initially, the Argo-1 has a total of 186 profiles of temperature and salinity, while the Argo-2 has a total of 180 profiles. As part of the quality check, 6 profiles from Argo-1 and 4 profiles from Argo-2 are removed. The trajectory and the timing of the Argo floats are presented in Fig. 1.

MLD can be estimated from temperature and salinity (density) profiles using different methods. In the present study, MLD is estimated for individual profiles based on segment method (Abdulla et al. 2016). Segment method is capable of overcoming the possible short-range gradients within the mixed layer and is an efficient method to estimate reliable MLD. We have also compared the MLD based on temperature and density profiles in the region, and no significant difference is observed between the temperature-based and density-based MLD estimates throughout the year except for some profiles during late winter (February–March). The results in the present study are based on density-based MLD estimates.

The eddy center is located based on sea level anomaly data from satellite altimetry following Chelton et al. (2011). The seasons are considered as December to February (winter), March to May (spring), June to August (summer), and September to November (fall).

Table 1 Monthly mean temperature and salinity at the surface, 100 m, 200 m, and 500 m

	Temperature				Salinity			
	Surface	100	200	500	Surface	100	200	500
Jan	26.89	25.10	22.33	21.63	38.97	40.10	40.45	40.59
Feb	26.25	25.43	22.37	21.63	39.09	39.97	40.45	40.59
Mar	26.74	24.52	22.29	21.62	38.58	40.07	40.47	40.58
Apr	27.74	24.66	22.46	21.62	38.45	39.89	40.43	40.57
May	29.35	24.68	22.39	21.62	38.34	39.93	40.45	40.57
Jun	30.09	25.02	22.51	21.62	38.51	39.85	40.43	40.58
Jul	31.44	24.93	22.47	21.63	38.54	39.97	40.44	40.58
Aug	31.74	24.94	22.47	21.63	38.58	39.99	40.43	40.57
Sep	31.67	24.75	22.40	21.62	38.86	39.96	40.44	40.57
Oct	31.14	24.36	22.28	21.62	39.15	40.01	40.47	40.58
Nov	30.62	24.72	22.24	21.62	39.07	40.03	40.49	40.59
Dec	28.45	24.91	22.22	21.63	39.03	40.13	40.48	40.59

Results and discussion

Mean thermal and haline structure in the central Red Sea

The monthly evolution of thermal and haline structure in the central Red Sea is investigated using profiles from two Argo floats located in the central Red Sea. The shallowest depth measured in a profile ranges from 0 to 10 m, and therefore, the depth 10 m is considered as surface. The

Table 2 The seasonal mean of temperature and salinity at the surface, 200 m, and 500 m

	Season	Surface (~5 m)			200 m			500 m		
		Argo-1	Argo-2	Diff.	Argo-1	Argo-2	Diff.	Argo-1	Argo-2	Diff.
Temperature	Winter	27.13	27.27	−0.14	22.26	22.35	−0.09	21.63	21.63	0
	Spring	27.91	27.99	−0.08	22.4	22.37	0.03	21.62	21.62	0
	Summer	31.13	31.04	0.09	22.3	22.67	−0.37	21.62	21.63	−0.01
	Fall	31.08	31.21	−0.13	22.24	22.37	−0.13	21.62	21.63	−0.01
Salinity	Winter	38.99	39.07	−0.08	40.44	40.48	−0.04	40.56	40.61	−0.05
	Spring	38.46	38.46	0	40.43	40.47	−0.04	40.55	40.59	−0.04
	Summer	38.48	38.6	−0.12	40.44	40.43	0.01	40.56	40.6	−0.04
	Fall	39.03	39.02	0.01	40.45	40.48	−0.03	40.56	40.6	−0.04

monthly mean profiles of both temperature and salinity are shown in Fig. 2, and the average temperature and salinity in the surface, 100-m, 200-m, and 500-m depths are compared in Table 1.

The warming phase in the evolution of thermal structure is active from March to August (Fig. 2, Table 1), where the mean SST (sea surface temperature) recorded an increase from 26.7 °C (March) to 31.7 °C (August). The cooling phase commenced by October (31.1 °C) and existed until February (26.3 °C). The intensity of warming is higher during April–May and that of cooling during December–January. The evolution of haline structure shows a clear seasonality with a maximum SSS (sea surface salinity) in October (39.2 PSU) and a minimum in May (38.3 PSU). The annual variability in temperature and salinity at 100 m is 0.5 °C and 0.1 PSU, respectively, which is less than 1/4th of the surface. The thermal and haline variability below 200 m is very limited, where nearly constant temperature and salinity is observed at 500 m and below throughout the year. The findings are consistent with previous results from previous studies (Sofianos and Johns 2007; Albarakati and Ahmad 2013; Alsaafani et al. 2017).

From the analysis of individual profiles, the maximum SST recorded in the central Red Sea by Argo-1 and Argo-2 are respectively 32.05 and 32.07 °C while that of the minimum are respectively 25.67 and 25.39 °C. The maximum SSS recorded are respectively 39.62 and 39.49 PSU, while the minimum SSS observed are 37.91 and 37.60 PSU, respectively. Relatively small differences are noticed in the measured temperature and salinity data from Argo-1 and Argo-2. The observed difference is expected mainly due to the distance between two profiling spots.

Comparison between measurements from Argo-1 and Argo-2

A comparison of the seasonal mean temperature and salinity from Argo-1 and Argo-2 is shown in Table 2. The measurements from both the Argo floats are nearly equal with relatively small difference of less than or close to 0.15 °C.

A noticeable difference between eastern and western Red Sea is observed in the thermal and haline structure. The profiles from March to May 2016 are used to check the east-west difference when the Argo-1 and Argo-2 are located respectively in the eastern and western parts of the region. The western part is cooler and more saline than the eastern side by ~0.3 °C and by ~0.1 PSU, respectively, which are consistent with the previous measurements (Luksch 1898; Vercelli 1927; Morcos 1970). The SSE surface wind in the southern Red Sea during winter and the associated northward current generate a pileup of surface warm water in the eastern Red Sea. A clockwise circulation is generated at right angles to the wind

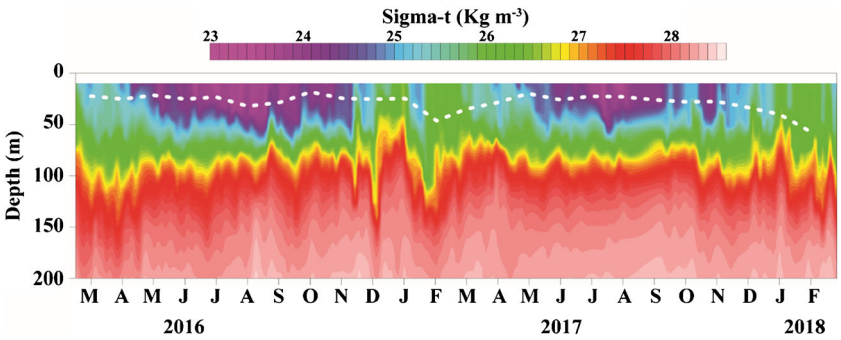

Fig. 3 Time-depth section of sigma-t for the upper 200-m layer from Argo-1

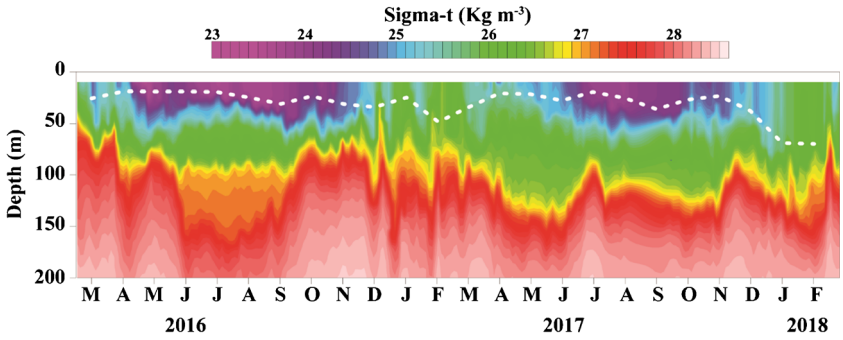

Fig. 4 Same as in Fig. 3, but for Argo-2

direction associated with the pileup of warm surface water in the eastern side and the upwelling of the westward moving deep water at the western side. This results in a cooler and more saline water in the western side compared to that of the eastern side (Thompson 1939; Morcos 1970; Robinson 1974; Alraddadi 2013). The above mechanism occurs almost all along the coastal region except the wind convergence zone, which is roughly between 18°N and 19°N (Zhai and Bower 2013; Abdulla et al. 2018).

The temporal evolution of MLD in the central Red Sea

The temporal evolution of MLD in the central Red Sea is examined using the density profiles from Argo floats. The MLD estimated for individual profiles Argo-1 and Argo-2 are shown in Figs. 3 and 4, respectively. The mixed layer in the central Red Sea is deeper during January–February and shallower during April–May months. The static stability of the water column is estimated and shown in Fig. 6, which increased from minimum value during February to its maximum during August coinciding with MLD variability. During summer, Argo-1 shows more stability than Argo-2 (Fig. 5).

In general, the mixed layer is deeper during winter associated with reduced stability and shallower during summer linked with increased stability. A close evaluation of individual profiles revealed that the presence of shallower MLD instances during winter and deeper MLD instances during summer. For example, Fig. 6 shows the profiles measured on 26 and 29 December 2016 by Argo-1 (red) and Argo-2 (blue)

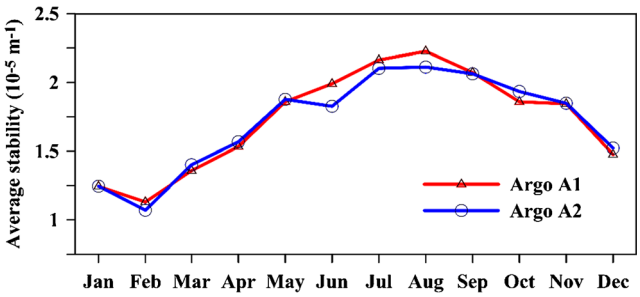

Fig. 5 Average static stability in the upper 200-m layer for Argo-1 (red) and Argo-2 (blue)

from nearby stations (distance < 50 km), which shows that the MLD recorded by Argo-1 is of the range 20 m, while that of Argo-2 is greater than 35 m. These differences might be attributed to factors controlling MLD variability. The contribution of each factor is investigated. The analysis shows that the wind and net heat flux are similar for both the Argo floats (figures not shown), while the sea level analysis displayed a significant difference.

The mean SLA from satellite altimetry for the period 23 to 29 December 2016 is shown in Fig. 6c. The positions of Argo floats during this period are marked over SLA. The results show that Argo-1 is located under the influence of a cyclonic eddy, while Argo-2 is located under the influence of an anticyclonic eddy. The cyclonic eddy resulted in shoaling of the mixed layer, while the anticyclonic eddy leads to the deepening of the mixed layer (Chelton et al. 2011; Hausmann et al. 2017; Abdulla et al. 2018). The difference in polarity of the eddies resulted in the observed MLD difference.

Observed difference from MLD climatology

The monthly mean MLD from Argo profiles is compared with the MLD climatology along the main axis of the Red Sea (Abdulla et al. 2018). The MLD climatology is prepared based on profiles from a verity of sources including CTD (conductivity-temperature-density profiler), XBT (expendable bathythermograph), MBT (mechanical bathythermograph), and PFL (autonomous profiling floats). The MLD climatology is restricted to the axial line of the Red Sea due to the insufficient data along the coastal region.

The comparison shows that the Argo MLD is matching well with that of climatology (Fig. 7a, b), where both datasets show deeper MLD during winter and shallower MLD during summer. However, in some of the months, the Argo-driven MLD has a relatively large deviation from the climatological MLD. Analysis based on sea level shows that the influence of local physical processes was the main reason for the observed difference. For example, consider two instances, (1) during December 2016 when Argo MLD is relatively lower than climatology and (2) during February 2018 when Argo MLD is relatively higher than the climatology.

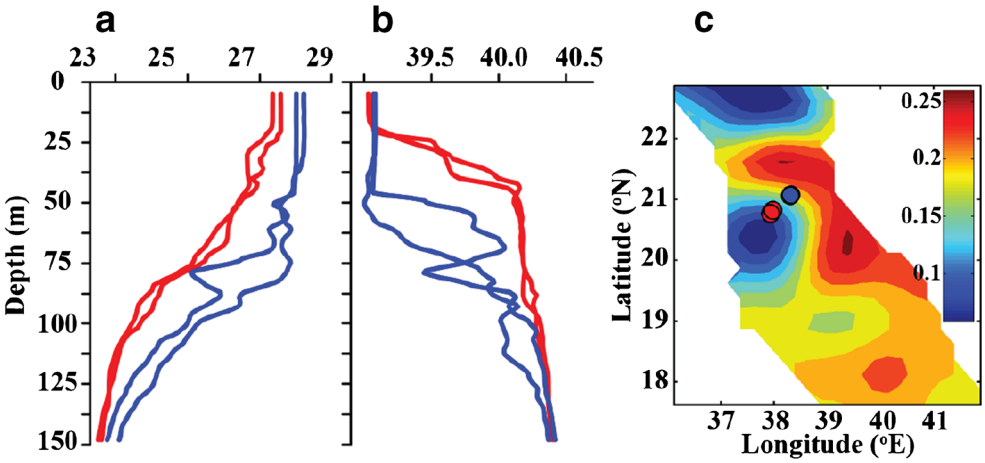

Fig. 6 The **a** temperature and **b** salinity profiles measured by Argo-1 (red) and Argo-2 (blue) recorded between 23 and 29 December 2016 and **c** the average SLA for the period 23–29 December 2016. The Argo float locations are marked on the SLA map

In the case of the first example, during December 2016, the MLD became shallower by the presence of a cyclonic eddy in the region (Fig. 8a). Similarly, in the case of the second example, during February 2018, the MLD became deeper by the presence of an anticyclonic eddy (Fig. 8b).

Summary and conclusions

The in situ temperature and salinity profiles from Argo floats are used to analyze the temporal variability of the thermal and haline structure of the central Red Sea and examine the MLD changes in the region. The seasonal variability is mostly limited to the upper 200-m water column, where the annual variability of the surface and 200-m depths are 5.4 and 0.25 °C respectively for temperature and 0.84 and 0.04 PSU for salinity.

The east-west difference in the thermal and haline structure in the region is analyzed using the profiles from March to May 2016, when Argo-1 and Argo-2 are located respectively in the eastern and western parts of the region. During this period, the western part is cooler and more saline than the eastern side by ~0.3 °C and by ~0.1 PSU, respectively.

The mixed layer in the central Red Sea is deeper during winter associated with a decrease in static stability of water column with deepest MLD in February. The shallowest mixed layer is observed in August where the static stability is at its maximum. The comparison with climatology MLD values shows that the Argo-based MLD pattern is in good agreement with that of climatology except during the presence of eddies.

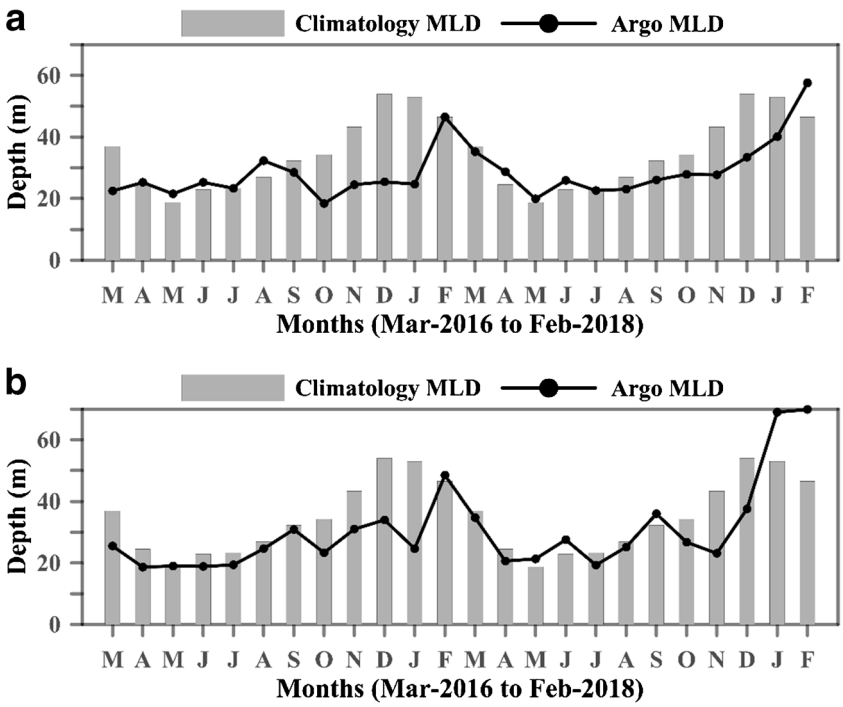

Fig. 7 **a** Comparison between the monthly mean MLD computed from the Argo profiles for Argo-1 (line) and the monthly MLD climatology (bar). **b** Same as in Fig. 8a, but for Argo-2

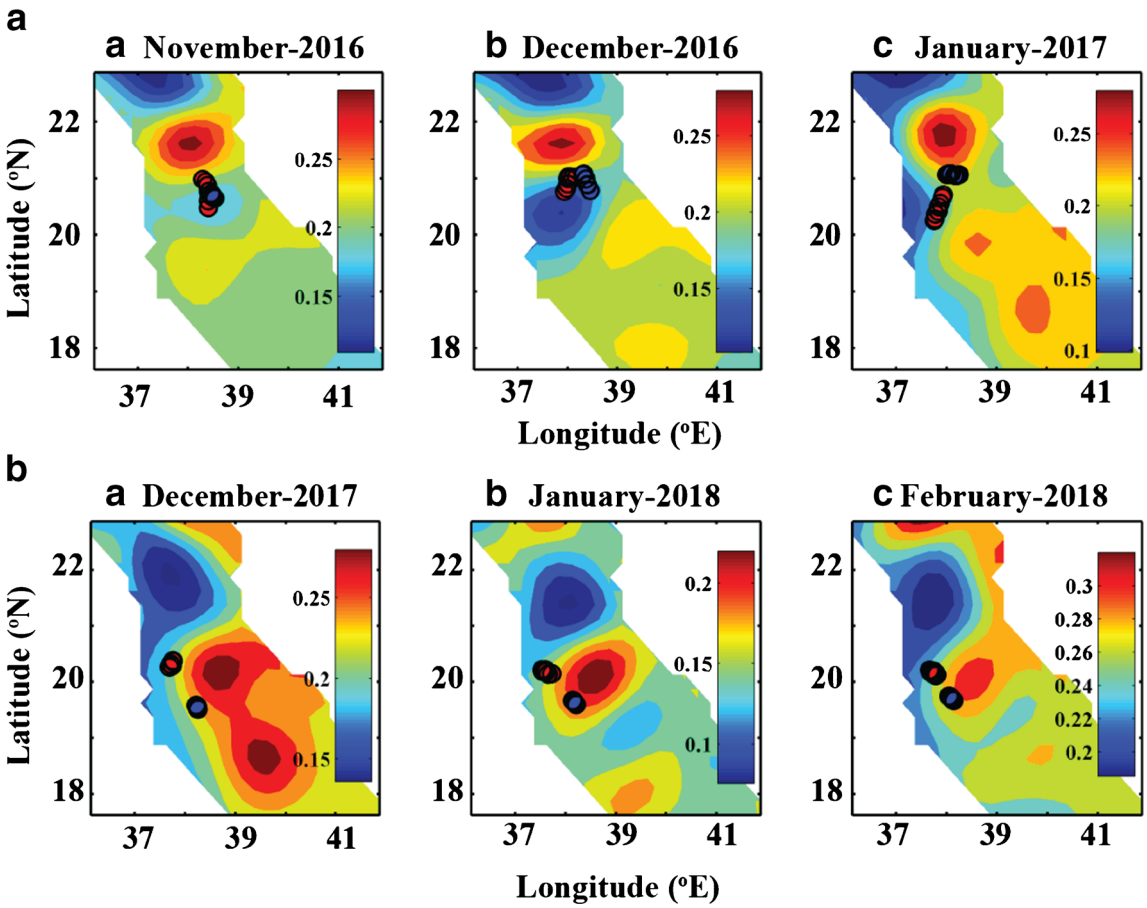

Fig. 8 **a** The monthly mean SLA from November 2016 to January 2017, overlaid with the Argo float location during the respective months (red and blue dots represent Argo-1 and Argo-2, respectively). **b** Same as in Fig. 8a, but for December 2017 to February 2018

During the presence of eddies, whether cyclonic or anticyclonic, a noticeable change is observed in the local mixed layer structure. The impact of eddies varies based on the static stability of the water column.

Argo observations are vital in investigating the dynamics of the ocean, especially in the remote regions. Since the oceanographic research in the Red Sea is limited due to scarcity of in situ datasets, with most of the measurements confined to the shipping channel, the availability of Argo profiles with wide spatial and temporal coverage is very helpful to understand the surface and subsurface physical and biological processes in the nearshore and offshore region. The advantage of available and ongoing in situ measurements in the Red Sea from Argo floats needs to be well exploited for observational and modeling studies of the region. At present, the Red Sea has a considerable number of profiles along the axis of the Red Sea, but not along the coast. In the future, we expect that the Argo floats will solve this issue to a large extent.

Acknowledgements The authors acknowledge the International Argo Program and the national programs that contribute to it for collecting the Argo profile data and making it freely available. The Argo Program is part of the Global Ocean Observing System (https://doi.org/10.13155/29825). The authors also acknowledge the AVISO data center for providing gridded sea level data (ftp://ftp.aviso.altimetry.fr/global/delayed-time/grids/msla/all-satmerged/h/).

Funding This project was funded by the Deanship of Scientific Research (DSR), King Abdulaziz University, Jeddah, under grant no. G-129-150-38. The authors, therefore, acknowledges with thanks the DSR's technical and financial support.

Declarations

Conflict of interest The author(s) declare that they have no competing interests.

References

Abdulla CP, Alsaafani MA, Alraddadi TM, Albarakati AM (2016) Estimation of mixed layer depth in the Gulf of Aden: a new approach. PLoS One 11:e0165136. https://doi.org/10.1371/journal.pone.0165136

Abdulla CP, Alsaafani MA, Alraddadi TM, Albarakati AM (2018) Mixed layer depth variability in the Red Sea. Ocean Sci 14:563–573. https://doi.org/10.5194/os-14-563-2018

Abdulla CP, Alsaafani MA, Alraddadi TM, Albarakati AM (2019) Climatology of mixed layer depth in the Gulf of Aden derived from

in situ temperature profiles. J Oceanogr 75:335–347. https://doi.org/10.1007/s10872-019-00506-9

Aboobacker VM, Shanas PR, Alsaafani MA, Albarakati AMA (2017) Wave energy resource assessment for Red Sea. Renew Energy 114:46–58. https://doi.org/10.1016/j.renene.2016.09.073

Albarakati AM, Ahmad F (2013) Variation of the surface buoyancy flux in the Red Sea. Indian Journal of Geo-Marine Sciences 42:717–721

Alraddadi TM (2013) Temporal changes in the Red Sea circulation and associated water masses. University of Southampton, Ocean and Earth Science, Doctoral Thesis, pp 198

Alsaafani MA, Alraddadi TM, Albarakati AMA (2017) Seasonal variability of hydrographic structure in Sharm Obhur and water exchange with the Red Sea. Arab J Geosci 10:315

Bessa I, Makaoui A, Agouzouk A, Idrissi M, Hilmi K, Afifi M (2020) Variability of the ocean mixed layer depth and the upwelling activity in the Cape Bojador, Morocco. Modeling Earth Systems and Environment 6:1345–1355

Chelton DB, Schlax MG, Samelson RM (2011) Global observations of nonlinear mesoscale eddies. Prog Oceanogr 91:167–216. https://doi.org/10.1016/j.pocean.2011.01.002

Chen D, Busalacchi AJ, Rothstein LM (1994) The roles of vertical mixing, solar radiation, and wind stress in a model simulation of the sea surface temperature seasonal cycle in the tropical Pacific Ocean. J Geophys Res 99:20345. https://doi.org/10.1029/94JC01621

D'Ortenzio F, Iudicone D, de Boyer Montegut C et al (2005) Seasonal variability of the mixed layer depth in the Mediterranean Sea as derived from in situ profiles. Geophys Res Lett 32:L12605. https://doi.org/10.1029/2005GL022463

Ducet N, LaTraon PY, Reverdin G (2000) Global high-resolution mapping of ocean circulation from TOPEX/Poseidon and ERS-1 and -2. Journal of Geophysical Research: Oceans 105:19477–19498. https://doi.org/10.1029/2000JC900063

Gaube P, McGillicuddy DJ Jr, Moulin AJ (2019) Mesoscale eddies modulate mixed layer depth globally. Geophys Res Lett 46:1505–1512

Gould J (2005) A beginners' guide to accessing Argo data. http://www.argo.ucsd.edu/Argo_Date_Guide.html

Hausmann U, McGillicuddy DJ, Marshall J (2017) Observed mesoscale eddy signatures in Southern Ocean surface mixed-layer depth. Journal of Geophysical Research: Oceans 122:617–635. https://doi.org/10.1002/2016JC012225

LaTraon PY, Dibarboure G (1999) Mesoscale mapping capabilities of multiple-satellite altimeter missions. J Atmos Ocean Technol 16: 1208–1223. https://doi.org/10.1175/1520-0426(1999)016<1208:MMCOMS>2.0.CO;2

Luksch J (1898) Expedition S. M. Schiff "Pola" in das Rothe Meer, Nordliche Halfte (Oct. 1895-May 1896). Wiissenschaftliche Ergebnisse. VI. Physikaische Utersuchungen (Expedition of the S. M. Boat "Pola" in the Red Sea, Northern Part (Oct. 1895 -May 1896). Scientific Res. Dtersuchungen Denkschr Akad Wiss (Math Nauturw KL)

Morcos SA (1970) Physical and chemical oceanography of the Red Sea. Oceanogr Mar Biol Annu Rev 8:73–202

Polovina J, Mitchum GT, Evans T (1995) Decadal and basin-scale variation in mixed layer depth and the impact on biological production in the Central and North Pacific , 1960-88. Deep-Sea Res 42:1701–1716

Robinson MK (1974) Atlas of monthly mean sea surface and subsurface temperature and the depth of the thermocline. In: L'oceanographie physique de la Mer Rouge, Symposium de l'Association Internationale des Sciences Physiques de l'océan. Paris: CNEXO. pp 29–54

Shanas PR, Aboobacker VM, Albarakati AMA, Zubier KM (2017) Climate driven variability of wind-waves in the Red Sea. Ocean Model 119:105–117. https://doi.org/10.1016/j.ocemod.2017.10.001

Sofianos SS, Johns WE (2007) Observations of the summer Red Sea circulation. J Geophys Res Ocean 112:1–20. https://doi.org/10.1029/2006JC003886

Sohail T, Gayen B, McC Hogg A (2020) The dynamics of mixed layer deepening during open-ocean convection. J Phys Oceanogr 50:1625–1641

Thompson EF (1939) Chemical and physical investigations. The exchange of water between the Red Sea and the Gulf of Aden over the "Sill." John Murray Expedition 1933–34. Scientific Reports 2:105

Vercelli F (1927) The hydrographic survey of the R. N. Amrairaglio Magnaghi in the Red Sea. Annual Hydrographic 2:1–290

Zeng L, Wang D (2017) Seasonal variations in the barrier layer in the South China Sea: characteristics, mechanisms and impact of warming. Clim Dyn 48:1911–1930. https://doi.org/10.1007/s00382-016-3182-8

Zhai P, Bower AS (2013) The response of the Red Sea to a strong wind jet near the Tokar Gap in summer. Journal of Geophysical Research: Oceans 118:422–434. https://doi.org/10.1029/2012JC008444

Zhan P, Subramanian AC, Yao F, Hoteit I (2014) Eddies in the Red Sea: a statistical and dynamical study. Journal of Geophysical Research: Oceans 119:3909–3925. https://doi.org/10.1002/2013JC009563